VOL. 11, NO. 19, OCTOBER 2016 ISSN 1819-6608
ARPN Journal of Engineering and Applied Sciences

www.arpnjournals.com

GEOCHEMICAL EXAMINATION OF THE MIDDLE-UPPER PERMIAN ROCKS, VOLGA RIVER REFERENCE SECTION

N. G. Nurgalieva, R. R. Khaziev, V. V. Silantiev, B. I. Gareev and G. A. Batalin
The Kazan Federal University, Institute of Geology and Petroleum Technologies, Russia
E-Mail: nurlit@yandex.ru

ABSTRACT

The Middle-Upper Permian rocks, Volga river reference section, were geochemically examined by XRF analysis to reveal the Ural provenance, aridity and humidity levels, smectite-illite association as indicator of environmental change. Geochemical variations correlate with the regional lithostratigraphic scheme and cyclicity.

Keywords: Permian rocks, XRF-data, chemostratigraphy

1. INTRODUCTION

The Permian basin of the Volga and Kama rivers region is known as a unique stratigraphic and palaeogeographical object formed in littoral, transition and continental environments controlled by interaction of tectonic factor, sedimentary influx, accommodation space and eustasy. We will consider the Urzhumian, Severodvinian and Vyatkian sediments within the Middle+Upper Permian sequence named as the Upper regional cycle, comprising the Ufimian, the Kazanian, the Urzhumian, the Severodvinian and the Vyatkian stages and horizons (~272-252,5 million years). The Urzhumian, the Severodvinian and the Vyatkian stages correspond to the range 265-252.5 million years (~ 13.5 Ma) [1].

The Upper regional cycle can be characterized as a cycle of second order corresponding to the supercycle or sequence and began his formation after the fifth global regressive phase of the Late Paleozoic. At the beginning of the formation of the Upper regional cycle most of the East European platform was a geological structure created by paleotectonic processes of Middle Carboniferous - Early Permian due to tectonic movements of the early Hercynian [2].

Hercynian Ural mountain structures were actively destroyed, and the eastern marginal area of the Russian plate was providing by a huge amount of clastic and chemogenic sedimentary material. Western boundaries of these formations are traced by marginal uplifts system of Tokmovsky vault. Waters of Boreal Permian Sea penetrated from north to Cisuralian foreland basin. Investigated Permian cycle acts as a foreland basin supercycle history from its opening until closing. Three megacycles corresponding to the Ufimian, Kazanian and Urzhumian+Severodvinian + Vyatkian stages occurred inside this supercycle.

According to lithofacies zonation proposed in [3] the Urzhumian and the Tatarian rocks of the Volga - Kama rivers area belong to the zone of carbonate-terrigenous coastal and lagoon sediments.

The mineralogical and chemical compositions of clastic sedimentary rocks are controlled by various factors, including the composition of their source rocks, environmental parameters influencing the weathering of source rocks, duration of weathering, transportation mechanisms of clastic material from source region to depocenter, depositional environment, and post-depositional processes. A lot of investigations are substantiating the above aspects pertaining to genesis of both ancient and modern siliciclastic sediments; the identification of palaeotectonic settings of provenance based on geochemical signatures of siliciclastic rocks (e.g. [4-15]). Among the terrigenous sedimentary rocks, clayey sediments (shales) are considered to represent the average crustal composition of the provenance much better than any other siliciclastic rocks. Shales retain most of the mineral constituents of the source and their bulk chemistry preserves the near-original signature of the provenance and more faithfully reveal palaeoweathering conditions [16].

The present work examines the geochemistry of sandstones, shales and limestones of the Monastery Ravine on the Volga River after geochemical investigation of the Urzhumian sediments in the neighboring outcrop of Cheremushka [17].

2. GEOGRAPHICAL SETTING AND GEOLOGICAL FIELD DESCRIPTION

The Monastery Ravine is located on the right bank of the Volga River, in the vicinity of the villages of Monastyrskoye and Il'inskoe (Figure-1). The outcrops M01-M18 (Figure-1) in the thalweg and slopes of gullies represent one of the most complete and readily accessible sections of the Biarmian and Tatarian series in the region of the Kazan Povolzhye [18]. The Monastery Ravine section was divided the section into 5 formations according to lithological criteria [18]. Recent studies, carried out on the section, followed after revised works, new sampling and supplement investigation [18].

According to the Resolution of Russian Interdepartmental Stratigraphic Committee, the Monastery Ravine section is a stratotype of the Urzhumian and a limitotype of the Severodvinian stages [18]. The section is represented there by all three stages -Urzhumian (~ Wordian), Severodvinian (~ Capitanian), Vyatkian (~ Wuchiapingian) - and the five formations of total thickness 150-180 m.

Urzhumian. The Urzhumian stage includes three formations: the First (I), the Second (II) and the most part of the Third (III) formations.

The formation I is composed of red-bed shales and is distinctly subdivided into two parts [18]. The shales of the lower part of the formation contain beds (3–20 cm thick) of grey and pink marls, rarely of brown siltstones and sandstones. In the upper part of the formation, shales are more homogenous and have a few beds of terrigenous and carbonate rocks. The shales often bear thin lenses of palygorskite.

Fossils occur rarely in the formation and mostly in its upper part. The first bed with fossils lies 10 m below the top of the formation and is composed of reddish-brown thinly bedded shales containing small (3–4 mm) distorted valves of conchostracans. Seven meters above this bed, dull-red imbedded shales, along with conchostracans, contain the isolated scales of the fishes *Platysomus biarmicus* Eichw., *Kargalichthys efremovi* Minich, *Amblypterina (Eurynotoides) costata* (Eichw.), *Acrolepis rhombifera* Eichw., *Palaeoniscum* cf. *kasanense* Gein. et Vetter, *Palaeoniscum* cf. *freislebeni* Bl., *Palaeoniscum kurtum* Krotov, *Varialepis orientalis* (Eichw.), *Varialepis bergi* A. Minich, *Elonichthys* sp., *Eurysomus* sp., and *Xenosynechodus* sp. The scales are 2–5 mm in size, black, not oriented and regularly distributed in the rock [18].

The formation II contains argillaceous-carbonate members [18]. These members are separated by two members of sandy-argillaceous rocks. The argillaceous-carbonate members are composed of greenish and pinkish-grey argillaceous carbonate rocks (0.2–1.5 m thick), containing thin (usually 10–30 cm) bands of red shale. The sandy-argillaceous members are composed of reddish-brown shales and siltstones with lenticular beds of brownish sandstones (up to 2 m).

Fossils are represented by non-marine ostracods, bivalves, fishes, amphibians, and plants. The bed of the greenish-grey siltstone (5–20 cm), 6.5 m above the base of the formation, contains numerous scales of the fishes *Platysomus biarmicus* Eichw., *Amblypterina (Eurynotoides) costata* (Eichw.), *Amblypterina (Eurynotoides)* sp., *Palaeoniscum* cf. *kasanense* Gein. et Vetter, *Palaeoniscum* sp., *Varialepis bergi* A. Minich, *Elonichthys* sp., *Eurysomus* sp., and *Xenosynechodus* sp. The large (0.5–3.0 cm) reddish-brown scales occur parallel to the bedding planes and mainly concentrate in the thin (3–5 mm) bed, which also yields small amphibian bones [18].

Eight meters below the top of the formation, the bed (0.1 m) of reddish-brown evenly and thinly laminated shale contains molds of the ostracods *Palaeodarwinula* cf. *fragiliformis* (Kash.), the bivalves *Palaeomutela castor* (Eichw.), *P. doratioformis* (Gus.), *Prilukiella subovata* (Jones), scales of the fishes *Varialepis* cf. *orientalis* (Eichw.), *Platysomus* sp., *Elonichthys* sp., fragments of the small-leafed plant *Phylladoderma tscheremushca* Esaul., and the remains of *Paracalamites frigidus* Neub. and *Stomochara diserta* Kis.[18].

The formation III is composed of reddish-brown shale and siltstones that are usually intercalated by thick lenses of yellowish-brown, obliquely laminated sandstones [18]. Carbonate rocks are represented by grey, nodular, and muddy limestones and marls. Different levels within the formation contain the remains of non-marine bivalves, ostracods, conchostracans, fishes, and tetrapods, and imprints and fragments of plants. Grey and brown siltstones 1–1.5 m above the base of the formation contain coaly remains of the trunks of *Sphenophyllum stouckenbergii* (Schm.) and *Paracalamites frigidus* Neub.[18].

The bed of reddish-brown and greenish-grey siltstone eight metres higher than the previous one contains the ostracods *Palaeodarwinula elongata* (Lun.), *P. chramovi* (Gleb.), *P. teodorovichi* (Bel.), *P. fainae* (Bel.), *Prasuchonella nasalis* (Shar.), and *P* cf. *stelmachovi* (Spizh.), the bivalves *Palaeomutela ulemensis* (Gus.), *P. wöhrmani* Netsch., *P. numerosa* (Gus.), *P. marposadica* (Gus.) and *P. subparallela* Amal., rare scales of the fishes *Varialepis orientalis* (Eichw.) and *Amblypterina (Eurynotoides)* sp., and rare amphibian vertebrae. The argillaceous limestone, four metres above, contains the ostracods *Palaeodarwinula elongata* (Lun.), and *Prasuchonella nasalis* (Shar.), the remains of complete fishes *Platysomus biarmicus* Eichw., *Kargalichthys efremovi* Minich, *Varialepis bergi* A. Minich, *V. orientalis* (Eichw.), *Amblypterina (Eurynotoides) costata* (Eichw.), *Amblypterina (Eurynotoides)* sp., *Palaeoniscum curtum* Krotov, and *Xenosynechodus* sp., a few small bivalves of *Palaeomutela* sp. and conchostracans [18].

The Severodvinian stage includes almost the total formation IV.

The formation IV is represented by the alternation of shale, siltstones and sandstones with marls and limestones [18]. Sandstones together with shales and siltstones form argillaceous-sandstone members.

The formation contains few fossils. At the base of the formation, there are the ostracods *Suchonellina inornata* (Spizh.), *S. parallela* (Spizh.), *S.* ex. gr. *parvaeformis* (Kash.), *Prasuchonella nasalis* (Shar.), the charophytes *Cuneatochara vjatkensis* Kis. and *C. amara* (Said.). Upwards in the section, five meters below the top of the formation, the bed of bluish-grey marl, apart from the similar ostracod assemblage, contains large conchostracan shells, fragments of the bivalve *Palaeomutela* sp., scales of the fishes *Amblypterina (Eurynotoides) costata* (Eichw.), *Platysomus* sp., *Kargalichthys efremovi* Minich, and *Varialepis bergi* A. Minich. Ostracods occur in more calcareous part of the marl, whereas fish scales occur in more argillaceous part. The intermediate type of marl contains conchostracans and fragments of bivalve shells [18].

The formation V is represented by the member (10–15 m) of yellowish-brown obliquely laminated sandstones, with conglomerate lenses, consisting of fragments of local rocks. Sandstones frequently contain silicified lenses and beds of red-bed siltstones, shale and marls [18].

The lower part of the Formation (shale and marls) contains ostracods and fragments of bivalves. Ostracods are characteristic of the boundary beds of the Vyatkian and Severodvinian Horizons and represented by *Palaeodarwinula fragilis* (Schn.), *Suchonellina parallela*

(Spizh.), and *Volganella magna* (Spizh.), *V. laevigata* Schn. Sandstones contain bones of labyrinthodonts (*Dvinosaurus*), chroniosuchids (*Chroniosaurus*), leptorophids (*Raphanodon),* pareiasaurs (*Praelginia* and others) and numerous therapsids [18].

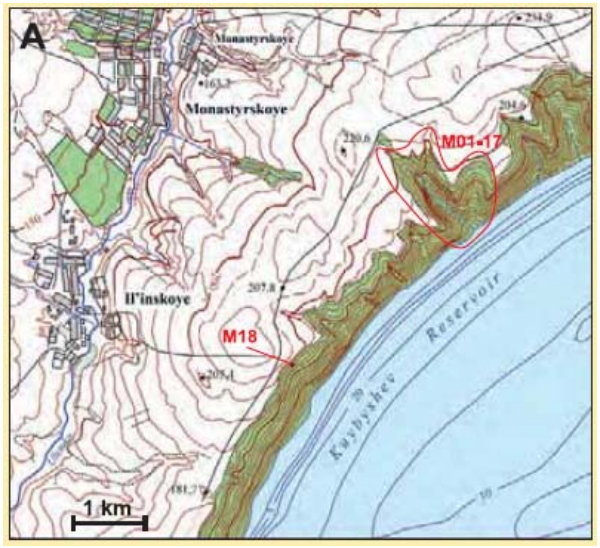

Figure-1. Geographical setting of object on [18].

3. MATERIALS AND METHODS

According to the field studies five formations are composed of clay, silt-sand, clay-carbonate facies.

In total 243 samples from all facies were analyzed. 192 samples are from clastic rocks and 51 samples are from carbonate rocks.

XRF spectrometry is an analytical laboratory technique used to detect the presence of specified elements in a sample material and subsequently determine the concentration of those elements present.

Bulk chemical analysis of samples was carried out using energy dispersive X-ray fluorescence method (EDXRF) on a fully-automated S2 RANGER (BrukerASX) spectrometer having Pd- tube as X-ray source and silicon drift detector.

Preparing of sample for analysis included its crushing in mill for 5 minutes to a particle size of about 40-50 μm; compaction with boric acid in a press with a force of 200 kN to get a tablet with a very smooth surface. Next, the tablet was placed in the instrument for analysis. The result can be received as a percentage of the components or in terms of their oxides in a concentration range from 100 % to ppm- level.

The analytical precession is better than 5% for major and trace elements.

The bulk mineralogy of clayey rocks was determined by X-ray powder diffraction (XRD) (Rigaku DMAXIII), using Nu-filtered Cu K α 15 kV - 40 mA instrumental settings. Clay mineralogy by XRD by using oriented samples after air-drying, saturation with ethylene glycol. The assignment of diffraction maxima was based on the standard International Centre for Diffraction Data (JCPDS).

4. RESULTS AND DISCUSSIONS

Samples are classified variously based on their chemical composition. They distribute in four geochemical facies after [19] (Figure-2).

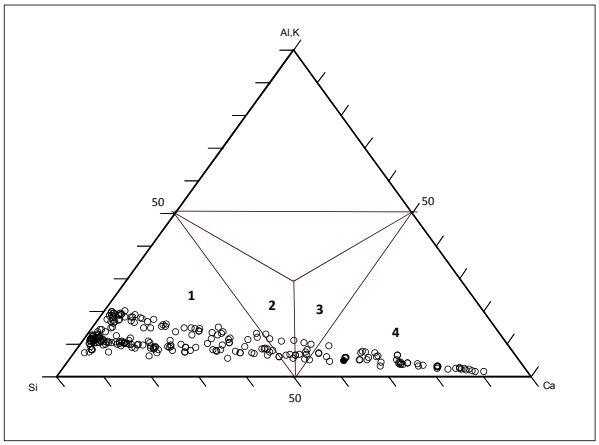

Figure-2. Distribution of samples on geochemical facies: 1- siliceous mudrock, 2 - mixed siliceous mudrock, 3- siliceous calcareous mudrock, 4 - limestone.

According to the scheme proposed by [20] in the bivariate log (Fe_2O_3/K_2O) versus log (SiO_2/Al_2O_3) diagram the samples plot in the field of mudstones (the formation I), wacke and litharenite (the formations II-V) (Figure-3a).

In the K_2O versus Na_2O bivariate diagram (after [21]) the samples of the present study plot essentially in quartz-rich field (Figure-3b). However, the samples have lower content of SiO_2 (average SiO_2 content 58,1%) in comparison with typical quartz-rich samples (average SiO_2 content: 89 wt % [21]).

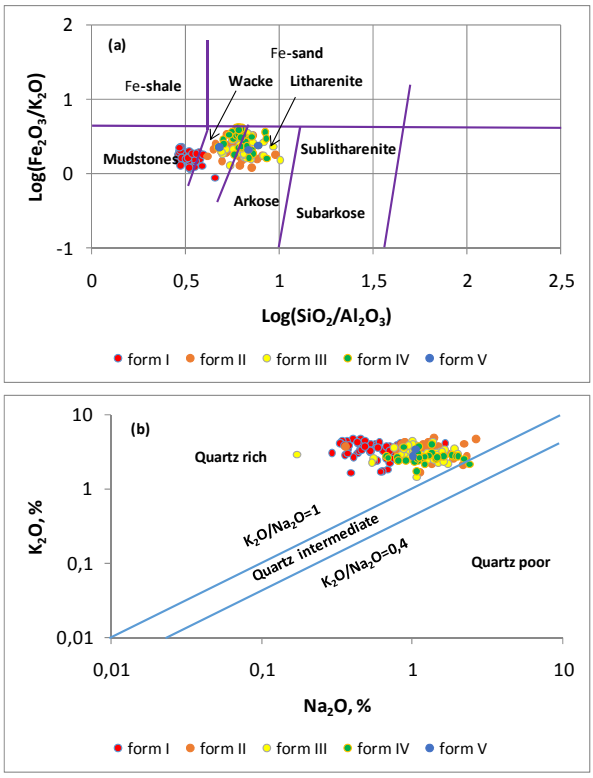

Figure-3. Geochemical classification of samples: (a) log (Fe_2O_3/K_2O) versus log (SiO_2/Al_2O_3) bivariate diagram. (b) K_2O wt. % versus Na_2O wt.% bivariate diagram.

It is known that the values of K_2O/Al_2O_3 of clays are less than 0.3 and the values of the same ratio of feldspars range from 0.3 to 0.9. By this ratio the samples of first formation correspond to clays range (ratio is less than 0.3) and second-fifth formations include both ranges. Therefore first formation is indicating by preponderance of clay minerals over K-bearing minerals such as K-feldspars and micas [22].

Samples were plotted in Al_2O_3 versus CIW diagram and in CIA versus ICV diagram (Figure-4a, b).

The CIW indicates that the particles derived or weathered from the source suffered sedimentary sorting (Figure-4a) and were deposited as sands, silts and clays after moderate degrees of weathering, while the ICV, used to evaluate the original composition of the sources of mudstones and siltstones (Figure-4b), illustrates the chemical effects of weathering of the potential source (near to andesite and basalt composition). Cr/V versus Y/Ni ratios are also used to identify sources. The studied samples plot between PAAS and ultramafic sources (Figure-5).

A high ICV value indicates compositionally immature source rocks riched in non-clay silicate minerals whereas low values represent compositionally mature source rocks. As weathering progresses, ICV values decrease due to conversion of feldspars to Al-bearing clays.

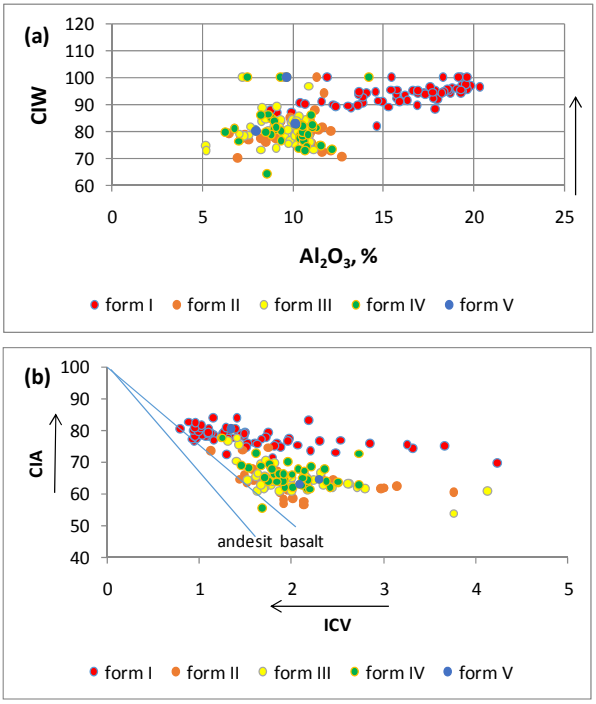

Figure-4. Relationship between weathering intensity and sedimentary sorting: (a) - CIW = [$Al_2O_3/(Al_2O_3 + CaO^* + N_2O)*100$] (Chemical Index Weathering [23]) versus Al_2O_3 and (b) - CIA = [$Al_2O_3/(Al_2O_3 + CaO^* + N_2O + K_2O)*100$] (Chemical Index of Alteration [5]) versus ICV = [$(Fe_2O_3 + MnO + MgO + CaO^* + N_2O + K_2O + TiO_2)/Al_2O_3$] (Index of Compositional Variability - [22]). CaO molar content is greater than that of Na_2O, therefore CaO* is assumed to be equivalent to Na_2O [24]. Arrows point on weathering increasing. ICV values for basalt are from [25] and for andesite from [26].

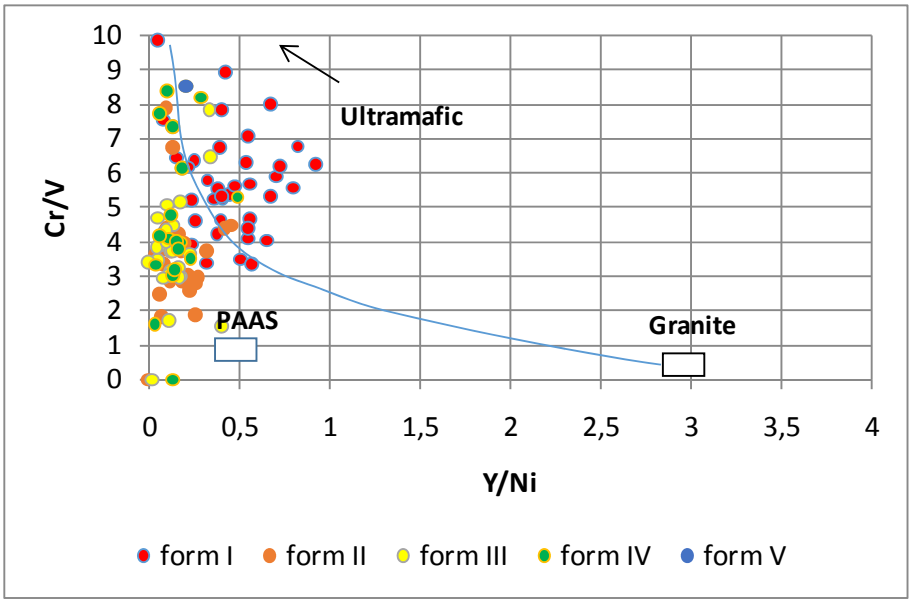

Figure-5. Cr/V versus Y/Ni diagram of samples after [27].

Al has a detrital and/or volcanic origin. In a marine environment Al a) may be adsorbed on biogenic silica that will be released upon dissolution [28; 29], b) may enter the oceans from rivers and be deposited on the seafloor in the form of amorphous Al-hydroxides adsorbed on other particles, c) may be released during alteration of fine-grained volcanic dust particles in the sediment [30].

Thus, variability in ICV values may be due to variations in source-rock composition, differences in weathering and alteration volcanic smectites and feldspars in the sediment [22].

Results of the XRD analysis indicate montmorillonite as the major clay mineral (Figure-6).

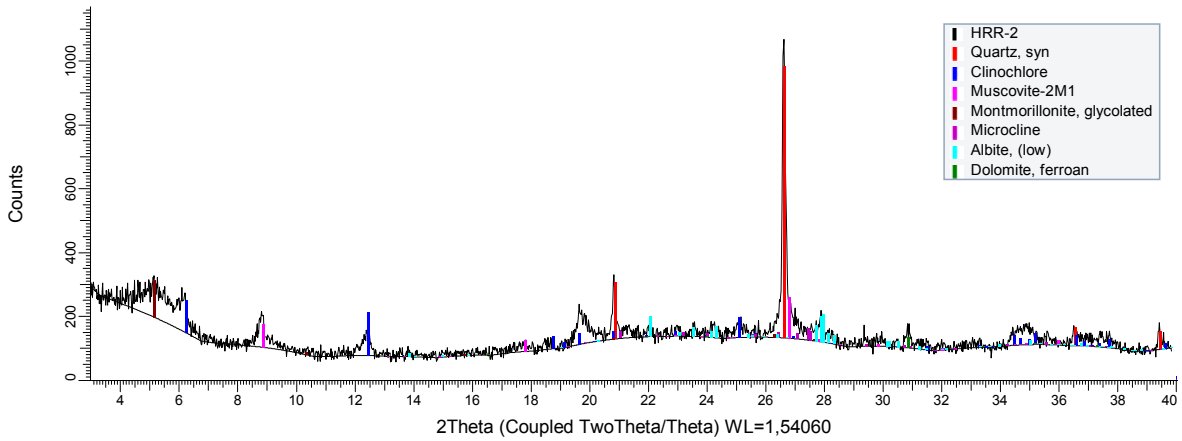

Figure-6. The typical XRD result of mudstone (formation 3).

Sample	Quartz(%)	Albite(%)	Mica(%)	Microcline(%)	Chlorite(%)	Dolomite(%)	Montmorillonite(%)	Sum
HRR-2	19,00	11,70	12,10	18,00	7,50	1,30	30,40	100,00

Normally, the source of illite, montmorillonite (smectite) and plagioclase is volcanic rocks [31; 32]. Chlorite can be result of weathering of tuffs and lapilies [13; 31; 33]. Early diagenetic temperature transformation of smectite into other phillosilicates can occur during sedimentation under the arid climate, the specific composition of provenance rocks, sharp and rapid changes in the hydrochemical composition of the sedimentary basin (by variation in Mg^{2+}) and clastic flows containing feldspars in the amount sufficient for enrichment of these

sediments with Al^{3+} and K^{+} through the biotic/abiotic processes at the stage of lithification [34]. Arid and semiarid climate of the middle and late Permian at the investigated area is specific condition that confirmed in SiO_2 % versus (Al_2O_3+K_2O+Na_2O) % diagram (Figure-7).

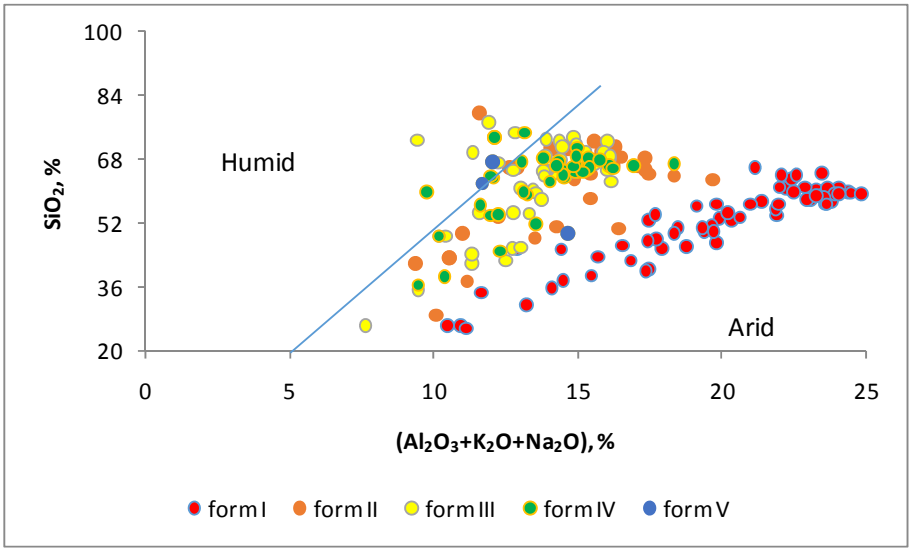

Figure-7. Chemical maturity of samples and their palaeoenvironment of deposition based on SiO_2 % versus (Al_2O_3+K_2O+Na_2O) % bivariate diagram after [8].

Tectonics setting of section is in favours of a passive continental margin (Figure-8).

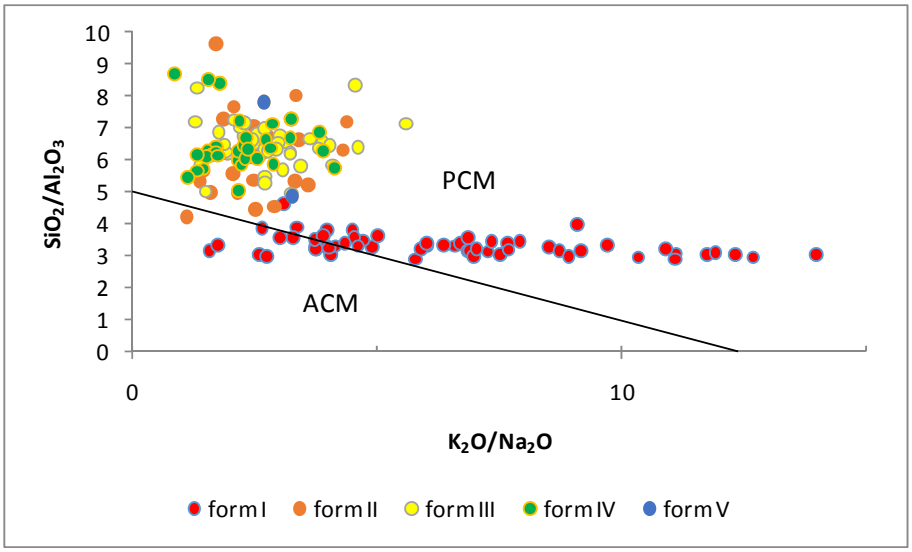

Figure-8. K_2O/Na_2O versus SiO_2/Al_2O_3 diagram (ACM - active continental margin; PCM - passive continental margin) after [35].

Plot on Figure-9 shows reliable relationships between elements. Contents of Al_2O_3, Fe_2O_3, TiO_2 increase and CaO and MgO decrease with increasing SiO_2. This suggests CaO and MgO mainly in carbonates, while other elements are associated with silicates. The content of Rb increases with the content of K_2O, which is typical of montmorillonite and illite [27]. MgO content decreases with increasing content of K_2O (for the first and second formations).

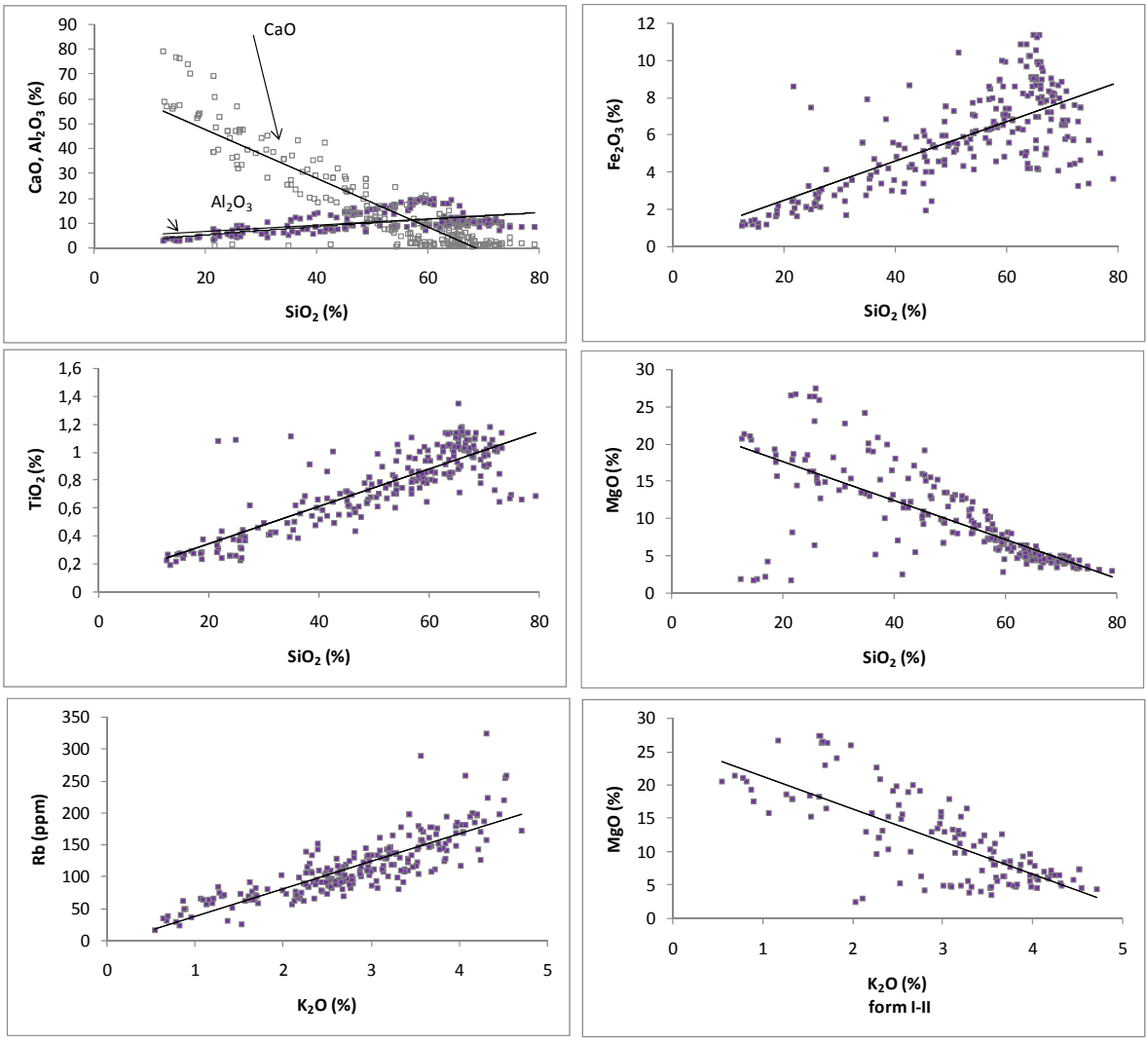

Figure-9. SiO_2vsCaO, Al_2O_3, Fe_2O_3, TiO_2, MgO diagrams and K_2O vsRb, MgO diagrams.

Figure-2, Figure-9, Figure-10 show that silica, aluminum, calcium, iron, magnesium, potassium play the main role in the geochemical rock composition. Figure-10 shows the variation of these elements with the increase of the total content. The cumulative amount of silica, aluminum, calcium is near and more than 80%. Variations of these components are also shown separately. By these variations 24 cycles are allocated. Polar behavior of silica and calcium control the boundaries of these cycles.

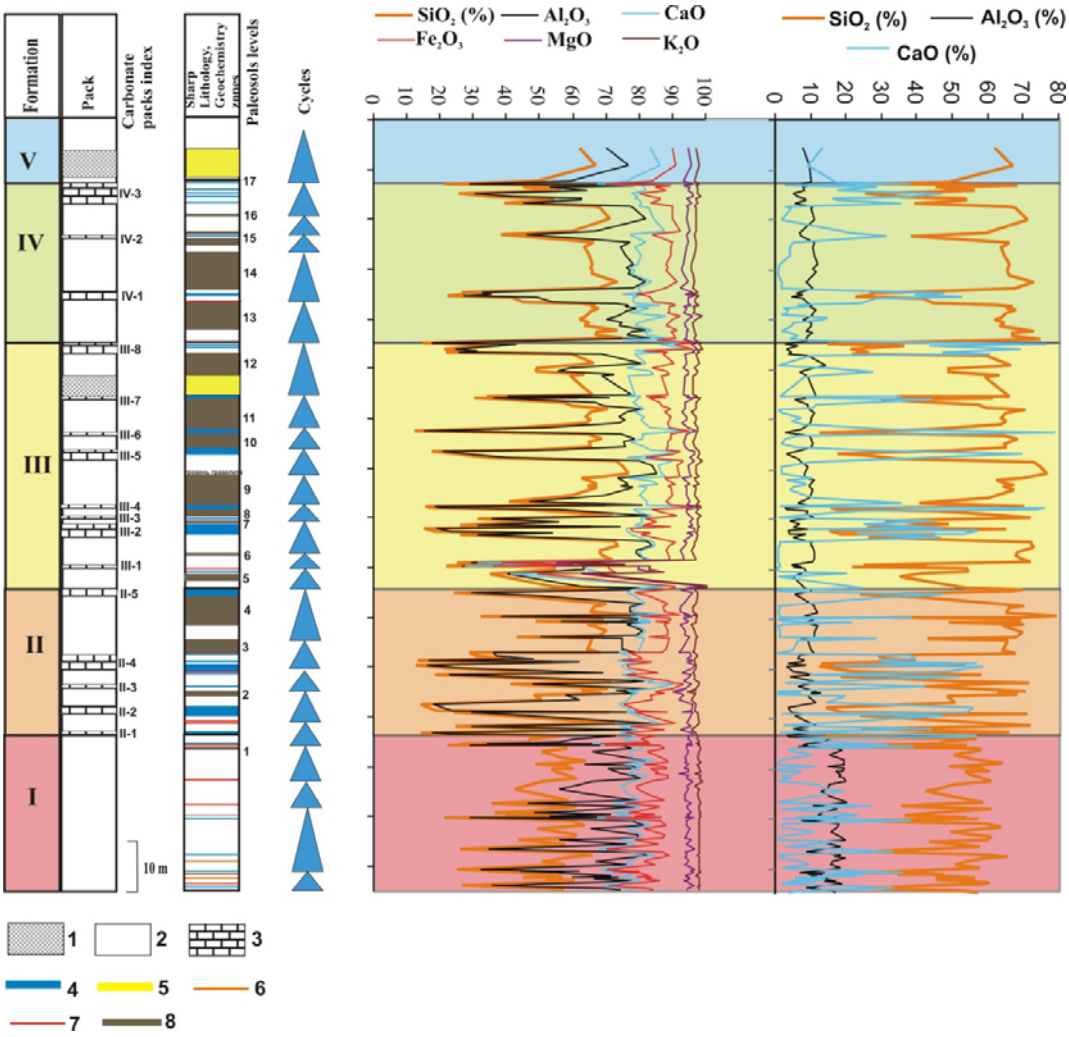

Figure-10. Main components variations (with cumulating and with no cumulating). Legends: 1- predominantly sandstones, 2- predominantly mudstones, 3- predominantly carbonate rocks. Sharp lithological levels: 4- carbonates, 5- sandstones, 6- palygorskite, 7- breccia, 8- pedosols.

Figure-11 demonstrates ratio K_2O/Al_2O_3 variation, indicating on a predominantly mudstone composition of formation I and wacke-litharenite composition of formations II-V. It is interesting polar behavior of K_2O and MgO variations in formations I and II (see also Figure-9). Negative correlations CaO, MgO versus SiO_2 point on a major role of carbonates in calcium and magnesium accumulation, wherein the magnesium increase (decrease potassium) is an indicator of an arid climate.

Orange arrows on Figure-11, Figure-12 sign the removal of potassium and addition of magnesium in the sedimentary system. Removal of potassium can be due to bacterial decomposition of silicate minerals (mica, soil minerals, feldspars) (bacteria produce organic acids, magnesium stimulates their activity (e.g. magnesium is associated with ATP)) so the orange arrows point on the arid climate, the increasing role of magnesium, increased bacterial growth, removal of potassium from mineral medium (decomposition of silicates) [36]. Aridization confirmed by the growth of the isotopic ratio of oxygen (evaporation of light isotopes of oxygen is enhanced in the sedimentary system is more than the heavy isotope), as well as growing and isotope ratio of carbon (isotopic data were taken from [18]), as falling productivity eukaryotes by the drop in grades Cu, Ni, Zn when changing the redox potential of the sediment (Mo content growth) (Figure-12) after [19]. Green arrows indicate humidity increase (role of fresh water flows and precipitation).

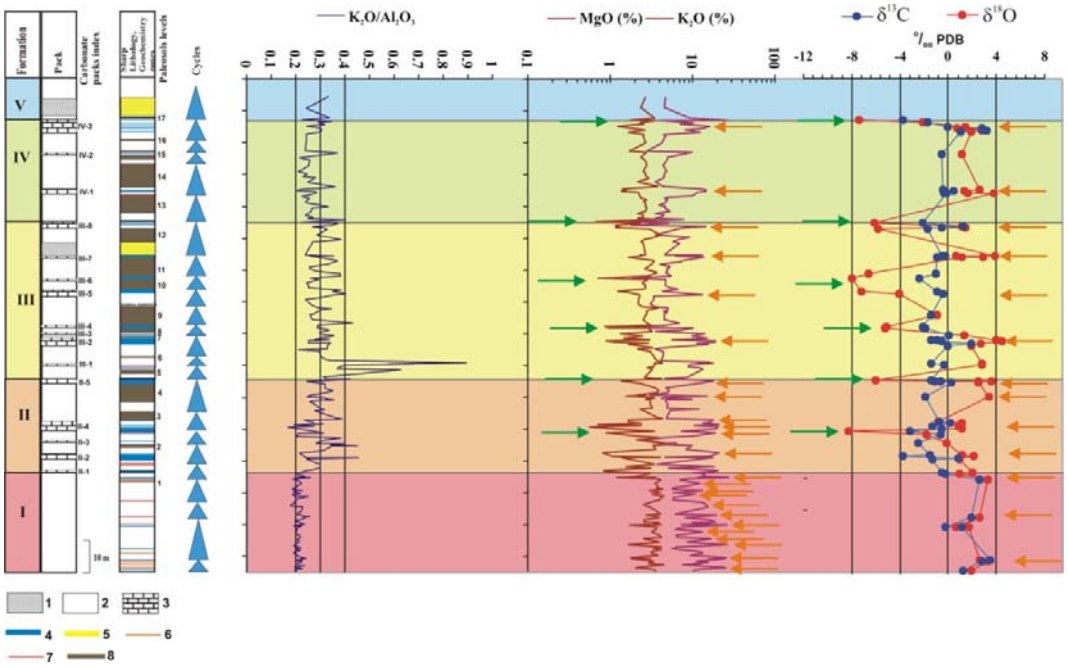

Figure-11. Potassium-aluminum-magnesium contents variations and isotopic data (data were taken from [18]) variations.

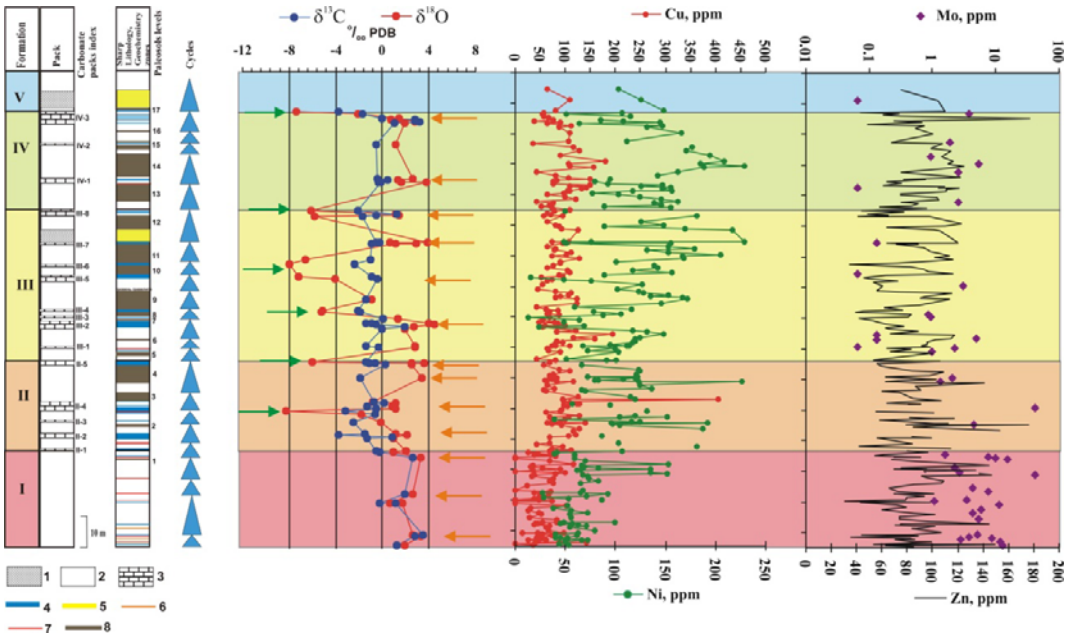

Figure-12. Isotopic data (from [18]) and geochemical terms of bioproductivity and redox-potential in sediment after [Baumgardner *et al.*, 2014].

Biologically controlled redox-potential causes smectite illitization. Bacterial decomposition of feldspars can be also source of Al^{3+} and K^{1+}[37; 34].

Figure-13 shows the position of geochemical data by the illite line and illite-rich facies line, where the first formation is most close to the illite-rich facies line.

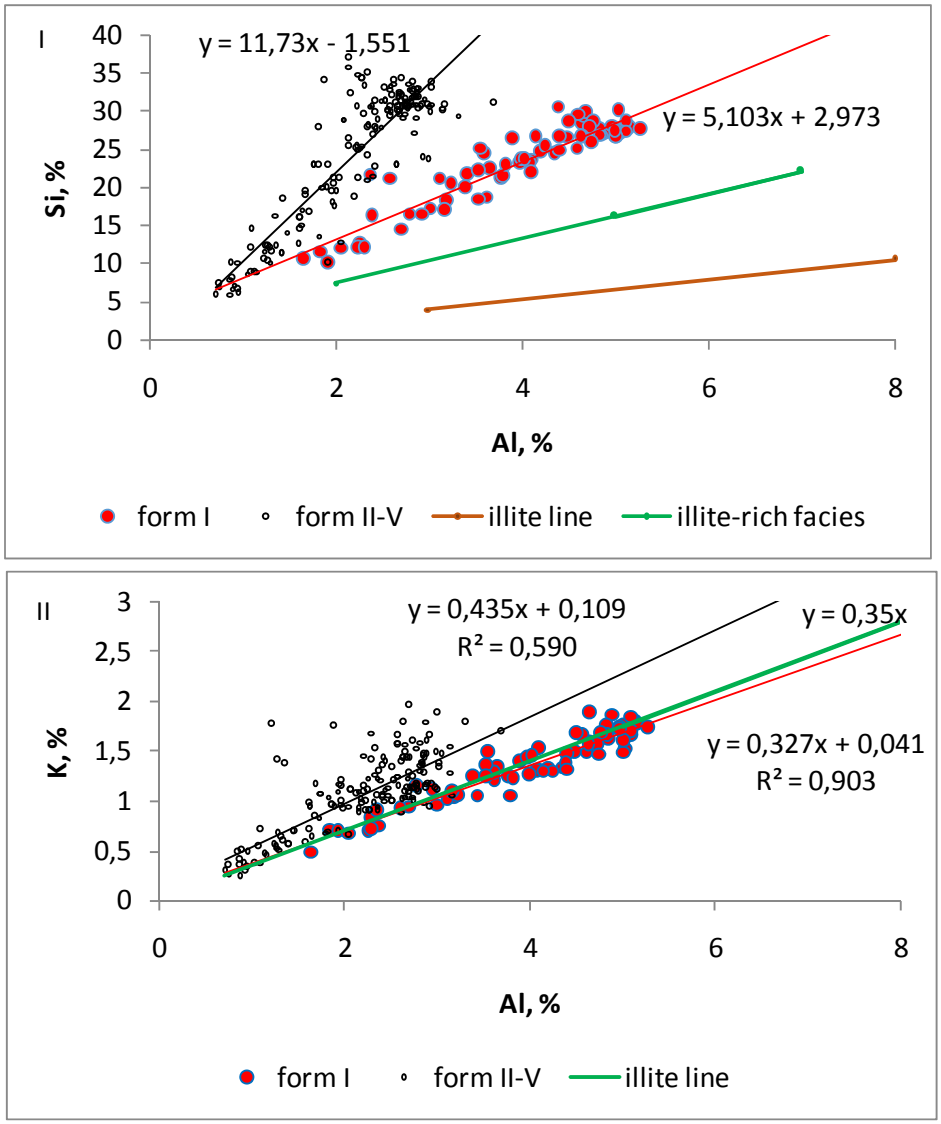

Figure-13. Geochemical plot by illite line on Si/Al=1.316:1 and illite-rich facies line on equation Si=2,939Al+1.52 (diagram I). On diagram II illite line is described by equation K/Al=0.35:1 (after [19]).

5. CONCLUSIONS

Geochemical data allow us to establish the specific nature of the Urzhumian and the Tatarian sediments in the east of the Russian plate, the right bank of the Volga River on the example of the reference section.

It was revealed the weathering trend of andesite-basalt rocks of Ural and terrigenous formations of Preuralian foreland.

Middle-Upper Permian sediments were accumulated in the arid climate (formation I) and semi-arid climate (formations II - V). Formation I (lower part of the Urzhumian stage) can be characterized as illite-rich facial succession.

Formations II-V were formed in conditions of a semi-arid climate, where significant arid periods alternated with periods of humidity increase and strengthen the role of freshwater flows and precipitation.

Clayey component is enriched by smectite that can be affected by varying degrees of low-temperature illitization controlled by relationship of potassium, magnesium, and fresh water inflow in the sediment. The behavior of this relationship in the section suggests the levels of aridity and humidity that are verified by isotope ratios of carbon and oxygen.

ACKNOWLEDGEMENTS

The financial support of the RFBR scientific research projects under 15-55-10007, 16-05-00706 project numbers and Russian Government Program of Competitive Growth of Kazan Federal University is gratefully acknowledged.

REFERENCES

[1] Nurgalieva N.G., Nurgaliev D.K. 2015. Cyclical composition of Permian rocks - ARPN JEAS. 10(1): 279-290. - http://www.arpnjournals.com/jeas/research_papers/rp_2015/jeas_0115_1452.pdf.

[2] Игнатьев В. И. 1976. Формирование Волго-Уральской антеклизы в пермский период.- Казань: Изд-во КГУ, 176с.

[3] Основные черты стратиграфии пермской системы СССР, отв. Редакторы КотлярГ.В., СтепановД.Л. - Л.: Недра, 1984, 280с.

[4] Potter P.E. 1978. Petrology and chemistry of modern Big River sands. J Geol. 86, pp.423-449.

[5] Nesbitt H.W., Young G.M. 1982. Prediction of some weathering trends of plutonic and volcanic rocks based on thermodynamic and kinetic considerations. J. Geol. 48, pp.1523-1534.

[6] Dickinson W.R., Beard I.S., Brakenridge G.R., Erjavec J.L., Ferguson R.C., Inman K.F., Knepp R.A., Lindber F.A. and Ryberg P.T. 1983. Provenance of North American Phanerozoic sandstones in relation to tectonic setting. Geological Society of America Bulletin. 93, pp. 222-235.

[7] Taylor, S.R. and McLennan S.M. 1985.The continental crust: its composition and evolution. Blackwell, London. p. 312.

[8] Suttner L.J., Dutta P.K. 1986. Alluvial sandstone composition and paleoclimate, I. Framework mineralogy. J Sediment Petrol. 56, pp. 329-345.

[9] Roser B.P., Korsch R.J. 1988. Provenance signatures of sandstone mudstone suites determined using discrimination function analysis of major element data. Chem Geol. 67, pp. 119-139.

[10] McLennan S.M., Hemming S., McDaniel D.K., Hanson G.N. 1993. Geochemical approaches to sedimentation, provenance, and tectonics. In: Johnsson M.J., Basu A., editors. Processes Controlling the Composition of Clastic Sediments. Boulder, CO, USA: Geological Society of America Special Paper.pp. 21-40.

[11] Юдович Я.Э, Кетрис М.А. 2008. Основы литохимии. Санкт-Петербург - «Наука», 480 с.

[12] Lee Y.I. 2002. Provenance derived from the geochemistry of late Paleozoic-early Mezozoic mudrocks of the Pyeongan Supergroup, Korea. Sedimentary Geology. 149, pp. 219-235.

[13] Potter P.E., Maynard J.B. and Depetris P.J. 2005. Mud and Mudstone: Introduction and overview. - Springer-Verlag Berlin Heidelberg.

[14] Zaid S.M. 2013. Provenance, diagenesis, tectonic setting and reservoir quality of the sandstones of the Kareem Formation, Gulf of Suez, Egypt. J. Afr. Earth Sci. 85, pp. 31-52.

[15] Nowrouzi Z., Moussavi-Harami R., Mahboubi A., Gharaie M.H.M., Ghaemi F. 2013. Petrography and geochemistry of Silurian Niur sandstones, Derenjal Mountains, East Central Iran: implications for tectonic setting, provenance and weathering. Arab J Geosci. 7, pp. 2793-2813.

[16] Pettijohn F.J. 1975. Sedimentary Rocks. 3rd ed. New York, NY, USA: Harper and Row.

[17] Nurgalieva N. G., Khaziev R. R., Gareev B. I. and Batalin G. A. 2014. Urzhumian stage in geochemical variations - ARPN JEAS. 5, pp.757-764.

[18] Mouraviev F.A., Arefiev M.P., Silantiev V.V., Balabanov Yu.P., Bulanov V.V., Golubev V.K., Minikh A.V., Minikh M.G., Khaziev R.R., Fakhrutdinov E.I., Mozzherin V.V. 2015. Monastery ravine section. Stratotype of the Urzhumian and limitotype of the Severodvinian stage - In: Type and reference sections of the Middle and Upper Permian of the Volga and Kama river regions. A field Guidebook of XVIII International Congress on Carboniferous and Permian. Kazan, August, 16-20, 2015 / D.K. Nurgaliev, V.V. Silantiev, S.V. Nikolaeva (Eds.)/ - Kazan: Kazan University Press.pp.120-141.

[19] Baumgardner R.W., Hamlin H.S., Rowe H.D. 2014. High-Resolution Core Studies of Wolfcamp/Leonard BasinalFacies, Southern Midland Basin, Texas - Search and Discovery Article #10607 (2014) - Posted June 30, 2014, adapted from poster presentation given at AAPG 2014 Southwest Section Annual Convention, Midland, Texas.

[20] Herron M.M. 1988. Geochemical classification of terrigenous sands and shales from core or log data. J. Sediment. Res. 58(5): 820-829.

[21] Crook K.A.W. 1974. Lithogenesis and geotectonics: The significance of compositional variation in flyscharenites (greywackes), J. Society of Economical, Paleontological and Mineralogical Special Publications. 19:304-310.

[22] Cox R., Lowe D.R., Cullers R.L. 1995. The influence of sediment recycling and basement coposition of evolution of mudrock chemistry in the southwestern United States. Geochim Cosmochim Acta. 59: 2919-2940.

[23] Harnois L. 1988. The CIW index; a new chemical index of weathering. Sediment Geol. 55, pp. 319-322.

[24] Shao J.Q., Yang S.Y. 2012. Does chemical index of alteration (CIA) reflect silicate weathering and monsoonal climate in the Changjiang River basin. Geology. 57(10): 1178-1187.

[25] Li Y.H. 2000. A Compendium of Geochemistry: Princeton, New Jersey, USA.

[26] Ewart A. 1982. The mineralogy and petrology of Tertiary-Recent orogenic volcanic rocks: with special reference to the andesitic-basaltic compositional range, in Thorpe, R.S., (Ed.), Andesites: Orogenic Andesites and Related Rocks: Chichester, U.K. John Wiley and Sons.pp. 25-95.

[27] Akkoca D.B., Kurum S., Huff W.D. 2013. Geochemistry of volcanogenous clayey marine sediments from the Hazar-Maden Basin (Eastern Turkey). Geologica Carpathica.64(6): 467-482.

[28] Hydes D.J. 1977. Dissolved aluminium concentration in seawater. Nature. 268: 136-137.

[29] [29] MacKenzie F.T., Stoffyn M. And Wollast R. 1978. Aluminium in seawater: control by biological activity. Science. 199: 680-682.

[30] Hein J.R, Hsuen-Wen Yeh Z. and Alexander E. 1979. Origin of iron-rich montmorillonite from the Manganese nodule belt of the North equatorial pacific. Clays and Clay Miner. 27, pp.185-194.

[31] Tucker M.E. 2001. Sedimentary petrology, Blackwell, London, U.K.

[32] Nichols G. 2009. Sedimentology and stratigraphy, Wiley-Blackwell, Chichester.p.419.

[33] Velde B. 1977. Clays and clay minerals in natural and synthetic systems, Elsevier.

[34] Khaziev R.R., Krinari G.A., Nurgalieva N.G., Gareev B.I., Batalin G.A. 2015. Some Aspects Concerning the Formation of Clayey Sediments of the Urzhumian Stage by the Geochemical Data on the Reference Section. Uchenye Zapiski Kazanskogo Universiteta. Seriya Estestvennye Nauki, 157(2): 106-117. (In Russian) http://kpfu.ru/portal/docs/F202968859/157_2_est_9_e.pdf.

[35] Roser B.P., Korsch R.J. 1986. Determination of tectonic setting of sandstone-mudstone suites using SiO_2 content and K_2O/Na_2O ratio. J. Geol. 94(5): 635-650.

[36] Кринари Г.А., Королев Э.А., Пикалев С.Н. 2003.Вулканокластическийматериал в палеозойской толще Татарстана: методы выявления и роль в нефтедобыче // Литосфера. № 1. С.27-38.

[37] Solotchina E.P., Prokopenko A.A., Kuzmin M.I., Solotchin P.A., Zhdanova A.N. 2009. Climate signals in sediment mineralogy of Lake Baikal and Lake Hovsgol during the LGM-Holocene transition and the 1-Ma carbonate record from the HDP-04 drill core. Quaternary International. 205: 38-52.